

# The subsurface radial gradient of solar angular velocity from MDI f-mode observations

T. Corbard and M. J. Thompson

*Space and Atmospheric Physics Group, The Blackett Laboratory, Imperial College, London SW7 2BW, UK*

**Abstract.** We report quantitative analysis of the radial gradient of solar angular velocity at depths down to about 15 Mm below the solar surface for latitudes up to  $75^\circ$  using the Michelson Doppler Imager (MDI) observations of surface gravity waves (f modes) from the Solar and Heliospheric Observatory (SoHO). A negative outward gradient of around  $-400\text{nHz}/R_\odot$ , equivalent to logarithmic gradient of the rotation frequency with respect to radius which is very close to  $-1$ , is found to be remarkably constant between the equator and  $30^\circ$  latitude. Above  $30^\circ$  it decreases in absolute magnitude to a very small value at around  $50^\circ$ . At higher latitudes the gradient may reverse its sign: if so this reversal takes place in a thin layer extending only 5 Mm beneath the visible surface, as evidenced by the most superficial modes (with degrees  $l > 250$ ). The signature of the torsional oscillations is seen in this layer, but no other significant temporal variations of the gradient and value of the rotation rate there are found.

## 1. Introduction

The velocity field of the rotational flow in the Sun's near-surface layers may play a significant role in small-scale dynamo action in that region and in the dynamics of supergranular convection. Surface observations over decades and even centuries have shown that the latitudinal variation of the surface rotation is rather smooth, being rather well described by a three-term (i.e. second-order) polynomial in  $\mu^2$  where  $\mu = \cos \theta$  and  $\theta$  is the colatitude. Recent analyses of high-resolution data, in particular those utilizing solar f-mode observations by the Michelson Doppler Imager (MDI) on board the Solar and Heliospheric Observatory (SoHO), have highlighted important departures from such a description of the rotation of the near-surface layers. The polar subsurface layers (i.e.  $\theta < 20^\circ$  and depths down to 28Mm below the surface) have been shown to be approximately 10nHz slower than expected from a simple three-term extrapolation from lower latitudes (Birch and Kosovichev, 1998; Schou et al., 1998; Schou, 1999); and Kosovichev and Schou (1997) have shown that, at a depth of 2 to 9 Mm beneath the surface, there exist zonal bands of alternate faster and slower rotation rate of  $\sim \pm 5\text{m/s}$  superimposed on the general trend described by the second order polynomial. This latter feature, inferred from the first observations of MDI in 1996, was found to be similar to the surface



© 2018 Kluwer Academic Publishers. Printed in the Netherlands.

‘torsional oscillations’ (Howard and Labonte, 1980) also observed in 1995 in Doppler measurements using the first GONG observations (Hathaway et al., 1996).) More recently still, analysis of both p and f modes from the GONG network and MDI instrument have further led to the conclusion that these banded structures extend at least down to 60Mm below the surface (Howe et al., 2000).

The observed f modes, being confined to the outer layers of the Sun, provide a relatively clean and straightforward measure of conditions there. But those results above that were obtained just from the f modes assumed at least implicitly that the angular velocity is not varying significantly with depth within the layer sensed by those modes. It is however well known that another important property of the subsurface layers is that they present a radial gradient of angular velocity. This was first suggested by the fact that different indicators such as Doppler shifts of photospheric Fraunhofer lines, various magnetic field features of different ages and sizes (sunspots, faculae, network elements,  $H_\alpha$  filaments) or the supergranular network, present different rotation rates (see the review of Howard, 1984; Schroeter, 1985; Snodgrass, 1992). This has been interpreted by assuming that the different magnetic features are anchored at different depths (e.g. Foukal, 1972; Collin et al., 1995), their different rotation rate being therefore interpreted as an indication of the existence of radial gradients of angular velocity in the subsurface layers. More specifically, noticing that the supergranular network rotation rate ( $\sim 473\text{nHz}$ ) was found to be  $\sim 4\%$  faster than the upper photospheric plasma rate obtained from spectroscopic methods and also  $\sim 2\%$  faster than various magnetic indicators thought to be rooted under the supergranulation layer, Snodgrass and Ulrich (1990) inferred that a maximum of angular velocity should exist somewhere between  $0.95R_\odot$  and the surface.

From the theoretical point of view, it has been suggested that the angular momentum per unit mass  $\Omega r^2 \sin^2 \theta$  could be conserved in the supergranular flow (Foukal and Jokipii, 1975; Foukal, 1977; Gilman and Foukal, 1979). From  $\partial\Omega/\Omega = -2\partial r/r$ , at fixed latitude, this simple argument leads effectively to a negative gradient below the surface, and the 4% difference in rotation rates would be explained if the supergranulation network velocity observed at the surface were reflecting the rotation rate at a depth of  $2\%R_\odot \simeq 15\text{Mm}$ , which turns out to correspond to the depth expected for the supergranular convection (Foukal, 1977; Duvall, 1980) (but see also Beck and Schou (2000) for more recent estimate). In order to reproduce the observed patterns of solar activity such as the equatorward migration of sunspots, early dynamo models based on a positive surface  $\alpha$ -effect indicated also that the angular velocity must decrease outwards i.e.  $\partial\Omega/\partial r < 0$  (e.g.

Leighton, 1969; Roberts and Stix, 1972). One of the first goals of helioseismology was therefore to test the assumptions about the negative gradient of angular velocity below the surface suspected from different surface observations. This was indeed first attempted by Deubner et al. (1979): although they did not resolve individual modes, they were able, from ridge-fitting separately the eastward- and westward-propagating near-equatorial waves in the  $(k, w)$  diagram, to detect such a negative gradient close to the surface. Subsequent helioseismic work using resolved mode frequencies has shifted much theoretical focus to the base of the convection zone by showing that the radial gradient of angular velocity in the bulk of the convection zone is weak and that a strong radial shear, the so-called tachocline, occurs at its base. The gradient  $\partial\Omega/\partial r$  is positive in the tachocline at sunspot (i.e. low) latitudes (Brown et al., 1989). This has led various dynamo theories to locate the dynamo action below the convection zone, with a negative  $\alpha$ -effect operating there (e.g. Gilman et al., 1989; Parker, 1993) though some recent work has revisited the idea of a positive surface  $\alpha$ -effect but invoking the action of a meridional circulation, equatorward below the convection zone and poleward at the surface, to produce the observed equatorward migration of sunspots by advective transport of flux (Dikpati and Charbonneau, 1999; Küker et al., 2001). The lack until recently of precise determinations of high-degree mode parameters made it difficult to obtain very localized inferences about the subsurface layers. But, because all the observed modes have amplitude close to the surface, inverters again got hints about the existence of a radial shear close to the surface (especially using methods such as regularized least-squares which readily extrapolate into regions where the data provide no localized information) though without being able to quantify precisely its extent and amplitude (e.g. Thompson et al., 1996; Corbard et al., 1997).

We show in this work that f-mode observations allow us to make quantitative inferences about the surface radial shear. These should be taken into account when modeling near-surface dynamo action or the dynamics of the supergranulation layer.

## 2. Observations

The data used here are 23 independent times series of 72 days obtained from the so-called MDI medium- $l$  program. These cover the period from 1996 May 1 to 2001 April 4 with interruptions during the summer 1998 (June 23 to October 23) and between 1998 December 4 and 1999 February 4 due to SoHO spacecraft problems. More details on the

production of these time series from the observations can be found in Schou (1999).

A given f-mode multiplet in the spectra comprises  $2l + 1$  frequencies  $\nu_{lm}$ , where  $l$  and  $m$  are the degree and azimuthal order of the spherical harmonic  $Y_l^m(\theta, \phi)$  describing the angular dependence of the modes. The so-called  $a$  coefficients for the multiplet are defined by the polynomial expansion:

$$\nu_{lm} = \nu_{l0} + \sum_{j=1}^{2l} a_j^l \mathcal{P}_j^{(l)}(m) \quad m = \pm 1, \pm 2 \dots \pm l \quad (1)$$

where  $\mathcal{P}$  are orthogonal polynomials normalized such that  $\mathcal{P}_j^{(l)}(l) = 1$  (Schou et al., 1994). All f modes considered here have degrees between  $l = 117$  and  $l = 300$  but the total number of multiplets observed is between 112 and 143, depending on the 72-day interval considered. For each observed mode, the central frequencies  $\nu_{l0}$  and the first 36  $a$  coefficients have been estimated using the method described in Schou (1992). Odd-indexed  $a$  coefficients, which describe the dependence of the frequencies that is an odd function of  $m$ , arise from the North-South symmetric part of the solar rotation. Even-indexed coefficients arise from latitudinal structural variation, centrifugal distortion and magnetic fields.

### 3. Data analysis

Following Ritzwoller and Lavelly (1991), we identify the North-South symmetric part of the angular velocity  $\Omega(r, \mu)$  with the odd-degree, zonal part of the toroidal component of a general stationary and laminar velocity field and write

$$\Omega(r, \mu) = \sum_{j=0}^{\infty} \Omega_{2j+1}(r) \bar{T}_{2j}^1(\mu), \quad (2)$$

where  $r$  is fractional radius and  $\bar{T}_{2j}^1 \equiv T_{2j}^1(\mu)/T_{2j}^1(0)$  are Gegenbauer polynomials (see Appendix) normalized such that the equatorial rate is given by the straight sum of the  $\Omega_{2j+1}(r)$ .

Assuming slow rotation, we can use a linear perturbation theory to predict the effect of rotation on the oscillation modes (e.g. Hansen et al., 1977). Moreover, with the polynomials  $\mathcal{P}$  and expansion Equation (2) as chosen, there is a one-to-one relation between odd  $a$  coefficients and the components  $\Omega_{2j+1}(r)$  (Ritzwoller and Lavelly, 1991), thereby reducing the full 2D problem to a set of 1D integral equations often

referred as the 1.5D problem. In the particular case of the f modes, we obtain

$$2\pi a_{2j+1}^l = u_{2j+1}^l \int_0^1 K_h^l(r) \Omega_{2j+1}(r) dr, \quad (3)$$

where the expression for the kernels  $K_h^l(r)$  and  $u_{2j+1}^l$  are derived in Appendix.

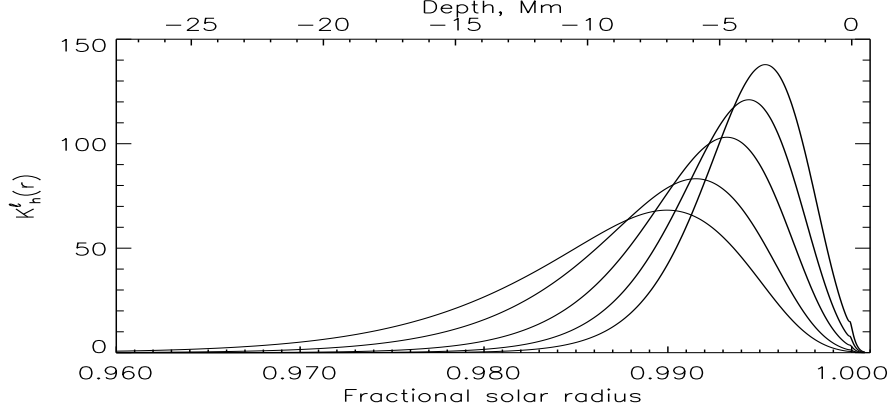


Figure 1. f-modes rotational kernels  $K_h^l(r)$  for  $l=117, 150, 200, 250, 300$  from left to right.

The 36  $a$  coefficients extracted from observation do not provide information about the terms above  $j = 17$  in the summation in Equation (2) and that corresponds to a limitation in the latitudinal resolution we can reach. Defining

$$b_{2j+1}^l \equiv \frac{2\pi a_{2j+1}^l}{u_{2j+1}^l}, \quad (4)$$

from Equations (2), (3) and (4) we obtain

$$\sum_{j=0}^{17} b_{2j+1}^l \bar{T}_{2j}^1(\mu_0) \approx \int_0^1 K_h^l(r) \bar{\Omega}(r, \mu_0) dr, \quad (5)$$

where  $\bar{\Omega}(r, \mu)$  refers to the part of the rotation profile corresponding to the sum Equation (2) truncated at  $j = 17$ . We can also show (Pijpers, 1997) that the above linear combination of  $b$  coefficients is such that

$$\sum_{j=0}^{17} b_{2j+1}^l \bar{T}_{2j}^1(\mu_0) = \int_0^1 \int_0^1 K_h^l(r) \kappa(\mu_0, \mu) \Omega(r, \mu) dr d\mu, \quad (6)$$

where  $\kappa(\mu_0, \mu)$  are the so-called latitudinal averaging kernels which show what latitudinal average of the true rotation rate is made at

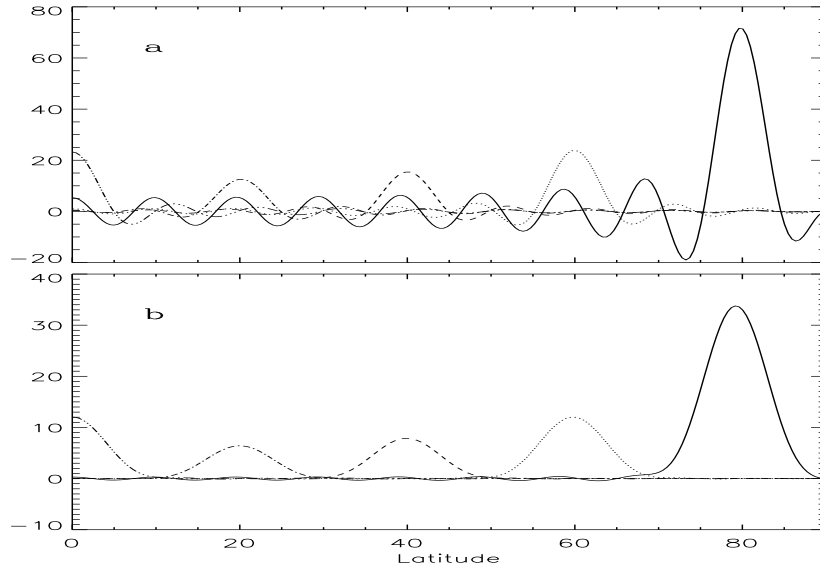


Figure 2. Latitudinal averaging kernels at 0, 20, 40, 60, 80° of latitude (double-dot-dash, dot-dash, dash, dot and full lines respectively) corresponding to the combination **a** Equation (8), **b** Equation (9).

each latitude. Figure. 2a shows that these kernels have their main peak centered at  $\mu_0$  but present an oscillatory behaviour which may lead to systematic errors if some small-scale features (corresponding to terms with  $j > 17$ ) exist in the true rotation rate. In order to avoid this, one may try to find instead the combination of  $b$  coefficients that leads to kernels that are optimally localized around a given latitude. This can be achieved following for instance the method of Backus and Gilbert (1968), but we notice here that a similar result can be obtained simply by introducing, in the sum of Equation (6), a correcting factor  $e^{-j(j+3/2)/l_0}$  where  $l_0 \equiv 117$  corresponds to the lowest degree of the observed f modes (see also Equation (15)). Doing this, the latitudinal averaging kernels are found better peaked (Figure 2b) and the formal errors associated with the linear combination of the  $b$  coefficients is lowered. Following the definition of Corbard et al. (2001), the latitudinal resolution obtained is about  $10^\circ$  at all latitudes.

The kernels  $K_h^l(r)$  associated with each f mode have a simple shape with only one maximum located at slightly different radial positions depending on the degree  $l$  (Figure 1). If we define  $r_0^l \equiv \int_0^1 K_h^l(r)rdr$ , the radial location of the center of gravity of these kernels, and assume a linear behaviour of the rotation rate at each latitude in the radial

domain where the f modes considered have appreciable amplitude, i.e.,

$$\Omega(r, \mu_0) = \alpha(\mu_0) - \beta(\mu_0)(r - 1) \quad (7)$$

in  $r > 0.97$ , say, we simply obtain

$$\sum_{j=0}^{17} b_{2j+1}^l \bar{T}_{2j}^1(\mu_0) \approx \bar{\Omega}(r_0^l, \mu_0), \quad (8)$$

where the meaning of  $\bar{\Omega}$  is the same as in Equation (5). Alternatively, a slightly modified choice of weights yields

$$\sum_{j=0}^{17} b_{2j+1}^l \bar{T}_{2j}^1(\mu_0) e^{-\frac{j(j+3/2)}{117}} \approx \langle \Omega(r_0^l, \mu) \rangle_{\mu_0} \approx \Omega(r_0^l, \bar{\mu}_0), \quad (9)$$

where the brackets denote the weighted average around  $\mu_0$ , the weighting function being the kernels of Figure 2b. The second approximate equality in Equation (9) would be exact if the rotation profile were a linear function of  $\mu^2$  in the domain covered by the averaging kernels (i.e.  $\pm 10^\circ$ ), with  $\bar{\mu}_0^2 \equiv \int_0^1 \kappa(\mu_0, \mu) \mu^2 d\mu$ ; the approximation is less good, however, at high solar latitudes.

The parameters  $\alpha$  and  $\beta$  can then be estimated at each latitude from a linear least-square fit, yielding not only an estimate of the value of the rotation rate at e.g. the surface, but also an estimate of the average gradient  $\partial\Omega/\partial r$  in the region sampled by the f modes. Finally we note that the dependence of  $\Omega$  as a function of radius in the near-surface layers may sometimes conveniently be described by a power of  $r$ : we note that this description is immediately derivable from our  $\alpha$  and  $\beta$ , since for small values of  $1 - r$  the right-hand side of Equation (7) is well approximated by  $\alpha(\mu_0)r^{-\alpha(\mu_0)/\beta(\mu_0)}$ .

#### 4. Results

By combining the frequency splittings within each f-mode multiplet in the manner given by Equation (8), for different choices of target latitude, we obtain measures of the near-surface rotation which are reasonably well localized in latitude and which correspond to different weightings in the depth direction. The latitudinal sensitivity is illustrated in Figure 2 and the depth sensitivity in Figure 1. Figure 3 shows the results of combining the data using Equation (8), averaged in time over all the datasets under study. In depth, the points are plotted at the center of gravity ( $r = r_0^l$ ) of the corresponding kernels (cf. Figure 1). It is evident from these results that, at low latitudes, the weighted rotation

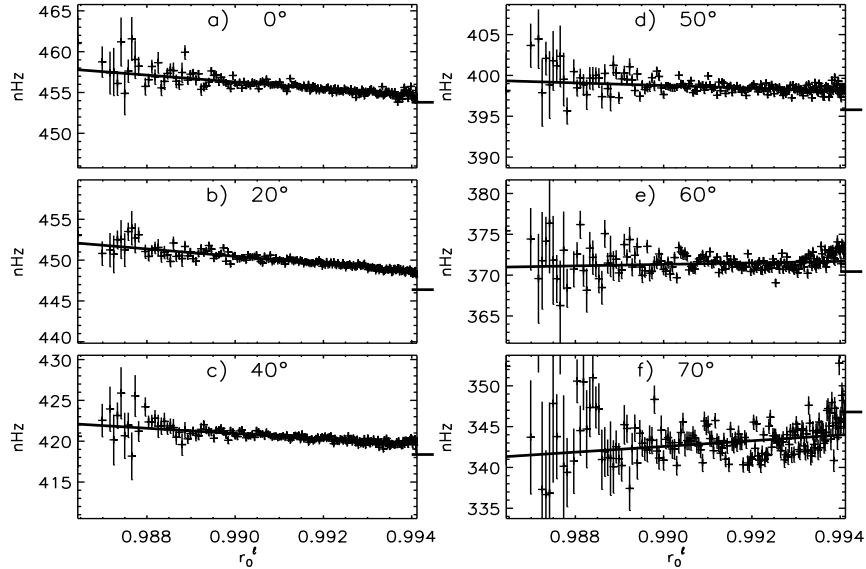
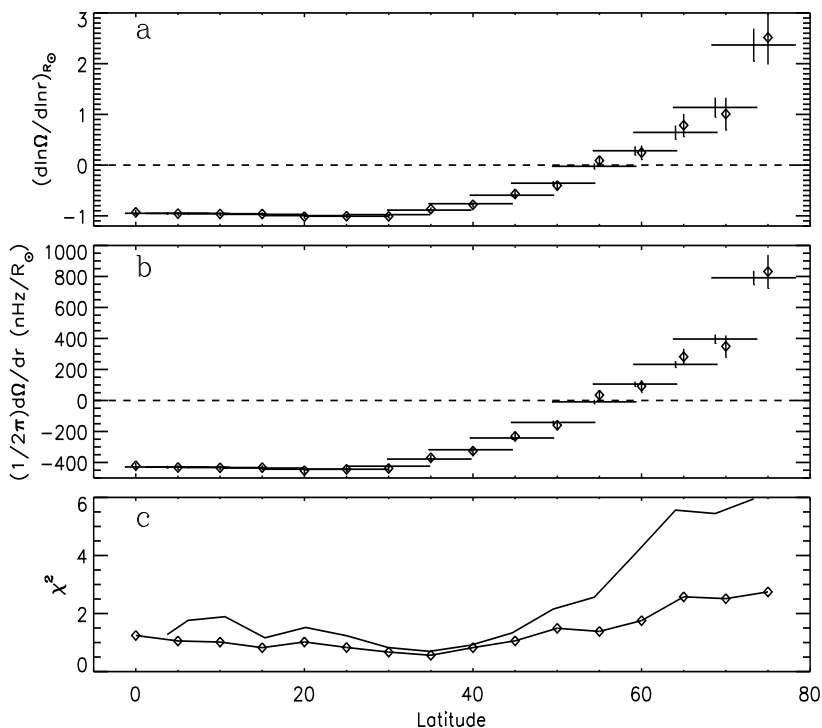


Figure 3. Time average of  $\bar{\Omega}(r_0^l, \mu_0)/2\pi$  (Equation (8)) for values of  $\mu_0$  corresponding to the latitudes indicated in each panel. The result of the linear fits (Equation (7)) are shown by the straight lines. The error bars are the standard deviation associated with the weighted temporal mean. The mark on the right of each panel indicate the surface plasma rate obtained by Snodgrass et al. (1984). Note that the surface spectroscopic value indicated on panel f is essentially an extrapolation from observations at lower latitudes.

increases with depth. If at each latitude separately we fit these results to a rotation profile that is linear in depth, we obtain the linear fits overplotted in Figure 3. These provide an average rotational gradient  $\beta(\mu_0)$  in the outer 15 Mm or so of the solar interior, and an extrapolated surface rotation rate  $\alpha(\mu_0)$ . The gradient, as a function of latitude, is presented in Figure 4, both in terms of its dimensional value and in terms of the logarithmic derivative  $\partial \ln \Omega / \partial \ln r$ . It may be seen that for latitudes below  $50^\circ$  the gradient of rotation with depth is negative; at about  $50^\circ$  it is close to zero; and for higher latitudes the average rotational gradient becomes positive. We note that the radial gradient is remarkably constant at latitudes up to  $30^\circ$ , and the value of the logarithmic derivative at these latitudes is close to  $-1$ . We return to this in the Discussion.

Another way to visualize the changing gradient with latitude is that in Figure 5, where we show the rotation rate extrapolated both to the surface ( $r = 1$ ) and to  $r = 0.97$ . The deeper rotation is faster than the surface rotation at low- and mid-latitudes, but slower at high latitudes. At low- and mid-latitudes the extrapolated surface rate agrees well with





*Figure 4.* **a** Logarithmic derivative of angular velocity as a function of latitude. This corresponds to the ratio  $\beta/\alpha$  of Equation (7). **b** Radial gradient of angular velocity  $\beta$  as a function of latitude. **c** Normalized  $\chi^2$  value of the linear fit. The diamond symbols are for the results obtained using Equation (8) while the other points are obtained using Equation (9). The horizontal error bars indicate the angular resolution as deduced from Figure 2b. The vertical error bars are formal errors deduced from the linear fit. The dashed horizontal line correspond to no radial gradient of angular velocity.

the spectroscopic surface measurements, given the approximately 1.5% spread in recent such determinations (see the review by Beck (2000)). For comparison, we have made a fit to our inferred surface rate below  $60^\circ$  latitude and present our fitting coefficients with the spectroscopic coefficients of Snodgrass et al. (1984) in Table I. Similarly to what has been found previously, our inferred rotation rate above  $70^\circ$  is markedly slower than what would be expected from a 3-term fit at low- and mid-latitudes: we return to this issue of the so-called ‘slow pole’ later.

Figure 4c shows the chi-squared for the least-squares fits at each latitude. The large chi-squared values at higher latitudes are striking. The difference between the chi-squared values when using equations (8) and (9) is also very noticeable: this arises largely because the error bars on

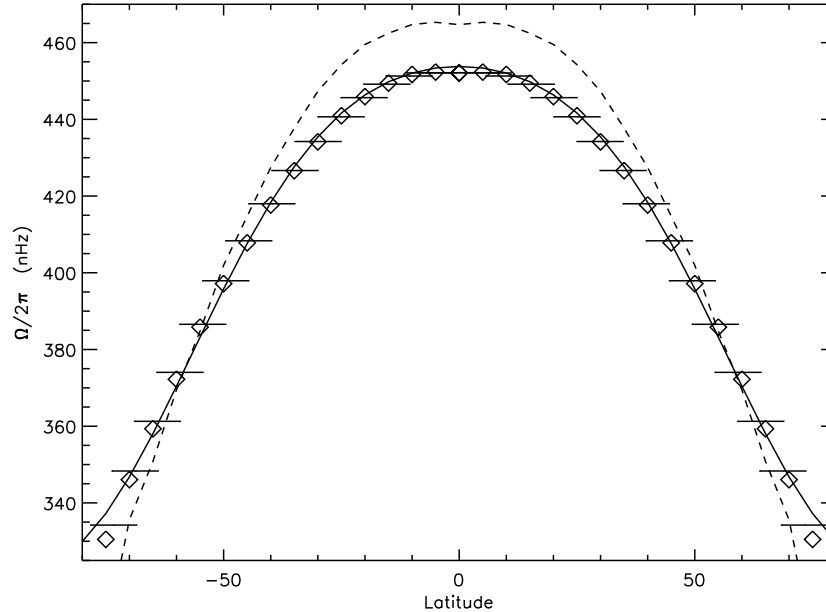


*Figure 5.* The full line gives the photospheric plasma rotation rate inferred by Snodgrass et al. (1984); the diamond symbols and horizontal bars correspond to  $\alpha$ , the intercept of the linear fit respectively in the case of Equation (8) and Equation (9) and the dashed line correspond to an extrapolation of the rotation rate at  $0.97R_{\odot}$  using Equation (7) in the case of Equation (8).

the fitted points are reduced by the exponential factor in Equation (9), which results in an increased chi-squared. Thus the interpretation of the absolute value of the chi-squared may be a little uncertain, but the trend with latitude for the two cases is similar. The higher values of chi-squared at higher latitudes is consistent with the greater deviation from a linear fit in the high-latitude panels of Figure 3. The systematic deviation of the near-surface points contributes most to the chi-squared: these correspond to the high-degree modes and so motivates taking a closer look at those data. (The scatter of the deepest points is large but less significant because of the large error bars on those points.)

We have therefore repeated our analysis but excluding those modes of degree  $l > 250$  and  $l < 160$ . The resulting gradient and chi-squared are shown in Figure 6. Compared with the previous result (Figure 4) the gradient is similar for latitudes lower than 50 degrees. Now it is evident from Figure 3 that, at high latitudes, excluding the high-degree modes will tend to make the fitted gradient less positive. Indeed, we find that the gradient without the  $l > 250$  data remains slightly negative up to about 75 degrees. Also, the values of chi-squared have been more than

Table I. Comparison between the surface plasma rate and our results from f modes analysis.

| Method   | $\Omega_1/2\pi$<br>(nHz) | $\Omega_3/2\pi$<br>(nHz) | $\Omega_5/2\pi$<br>(nHz) |
|--|--------------------------|--------------------------|--------------------------|
| Snodgrass et al. (1984) <sup>1</sup>                                   | 436.4                    | 21.0                     | -3.6                     |
| f modes ( $l$ -averaged) <sup>2</sup>                                  |                          |                          |                          |
| ( $117 \leq l \leq 300$ ) $\langle r_0^l \rangle = 0.991$ <sup>3</sup> | 438.8                    | 21.0                     | -3.9                     |
| ( $160 \leq l \leq 250$ ) $\langle r_0^l \rangle = 0.991$              | 438.9                    | 21.2                     | -4.0                     |
| f modes (surface extrapolation) <sup>4</sup>                           |                          |                          |                          |
| ( $117 \leq l \leq 300$ )  | 435.8                    | 20.2                     | -3.2                     |
| ( $160 \leq l \leq 250$ )  | 435.7                    | 20.5                     | -3.6                     |

<sup>1</sup>Spectroscopic measurements made at the Mount Wilson 150-foot Tower between 1967 and 1982.

<sup>2</sup>Average of the first 3 b coefficients (cf. Equations (4), (8)).

<sup>3</sup>Center of gravity of the corresponding  $l$  averaged radial kernels.

<sup>4</sup>Obtained by fitting the intercept  $\alpha(\mu)$  to the expansion Equation (2) for latitudes below  $60^\circ$ .

halved at high latitude, compared with our previous linear fit to all the f-mode data (Figure 6b). The inferred low- and mid-latitude surface rate is barely affected (compare the last two lines of Table I).

It is interesting also to compare the linear fit to the  $l < 250$  data with a fit of a constant function to the same data: the constant fit is equivalent averaging the f-mode splittings over  $l$  (see Table I). It is evident from Figure 6b (dotted line) that this provides a very poor fit below about  $55^\circ$ : the data strongly favour the model with a linear depth-dependence there. At high latitudes, the linear fit selects only a very small gradient and so the two chi-squared functions are very similar: the data for  $l < 250$  indicate that at high latitudes the gradient is small, in the range of depths spanned by their lower turning points.

If the data for  $l > 250$  are indeed reliable, then the discrepancy between the results in Figures 4a and 6a implies that the model of rotation varying linearly with depth is not appropriate at high latitudes and the extrapolation to the surface at those latitudes will be unreliable. An alternative approach is to attempt to construct kernels that are localized in depth using the Optimally Localized Averaging (OLA) kernel in depth (cf. Christensen-Dalsgaard et al., 1990) in the manner of (Backus and Gilbert, 1968). Such kernels at two selected depths are shown in Figure 7: they were constructed using all the available f modes. It should be noted that the method succeeds in producing kernels which are reasonably localized and which have their center of gravity outside the range of abscissa values in Figure 3, that is, the

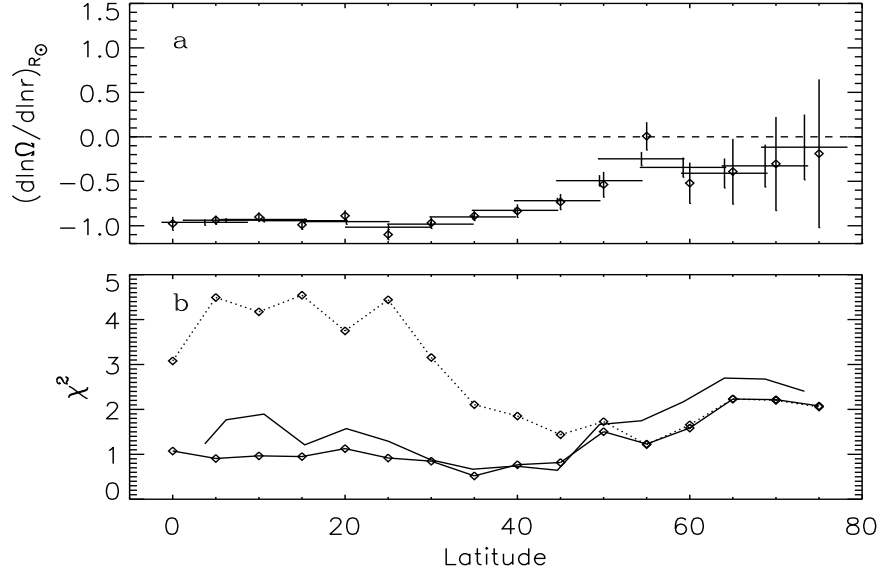
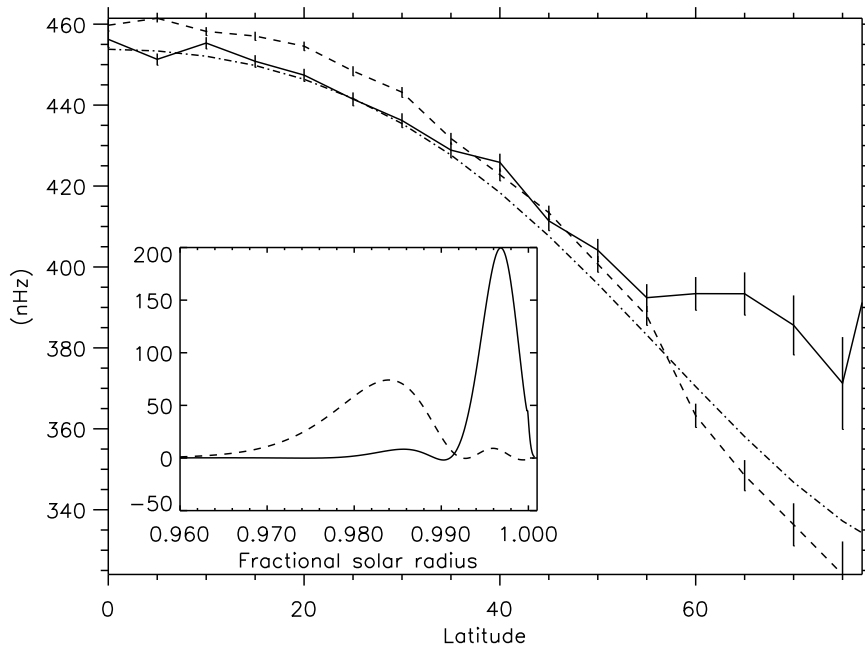


Figure 6. Similar to Figure 4 but using only modes  $160 \leq l \leq 250$ . The radial gradient of angular velocity remains negative even at latitudes above  $55^\circ$ . The dotted line on panel b shows, in the case of Equation (8), the  $\chi^2$  values corresponding to a fit by a constant which is equivalent of taking an average over  $l$ .

method uses the mode sensitivities to extrapolate to greater depths and closer to the surface. In particular, in the latter case one expects that the increasing trend of values for the near-surface points in Figure 3e,f means that the near-surface Backus-Gilbert inversion at those latitudes will have values higher than those seen in Figure 3. This is exactly what is found (Figure 7): the Backus-Gilbert inversion at high latitudes for  $r = 0.986$  interestingly falls below the 3-term spectroscopic surface rate, but even more strikingly the corresponding near-surface result at  $r = 0.997$  lies above it by 2–4 standard deviations. This is another way of demonstrating that the increasing values of the combined splittings for  $l > 250$ , if they are reliable, indicate a strongly positive gradient of rotation with radius in the rather superficial subsurface layers at high latitudes.

To look for possible temporal variations of the subsurface shear, we have analyzed each one of the 23 72-day datasets individually in exactly the same manner as we analyzed the time-averaged set (e.g. Figure 3), and derived an intercept value  $\alpha(\mu_0; t)$  (corresponding to the surface rate at that location and epoch) and slope  $\beta(\mu_0; t)$  from a linear fit to the combined splittings for each latitudinal location  $\mu_0$  and time  $t$ . The resulting estimated surface rates and slopes at three latitudes



*Figure 7.* Rotation profiles as a function of latitude corresponding to depth averaged shown in the sub panel. The dashed and full lines correspond respectively to the shallower and deeper kernels which have respectively  $0.986R_{\odot}$  and  $0.997R_{\odot}$  as center of gravity. The dot-dashed line corresponds to the Snodgrass et al. (1984) plasma rotation rate. These results are obtained by using all modes from  $l = 117$  to  $l = 300$ .

(equator,  $30^{\circ}$ ,  $60^{\circ}$ ) are shown in Figure 8. The large-scale variations in the surface rate correspond very well to the migrating banded zonal flows (torsional oscillations) measured by Schou (1999) and by Howe et al. (2000): the equatorial surface rate starts high because of the tail-end of one migrating band of faster flow, then drops down and rises again towards solar maximum as another band of faster flow reaches the equator: the latter was at  $30^{\circ}$  at the beginning of the cycle, hence the rate at that location starts high and drops as the band migrates closer to the equator. The  $60^{\circ}$  rate rises as the high-latitude banded flow reported by e.g. Schou (1999) strengthens towards solar maximum. The slope shows no significant corresponding variations, implying that the torsional oscillations raise and lower the rotation rate across the whole depth of the layer without changing the shear gradient. There are indications of annual variations in the inferred values of the slope (most strikingly at  $30^{\circ}$ ), which are almost certainly an artifact: such artifacts can conceivably arise from annual variations in SoHO's orbit. Other evidence for one-year artifacts in the f-mode data is presented by Antia et al. (2001). These should not affect the time-averaged values,

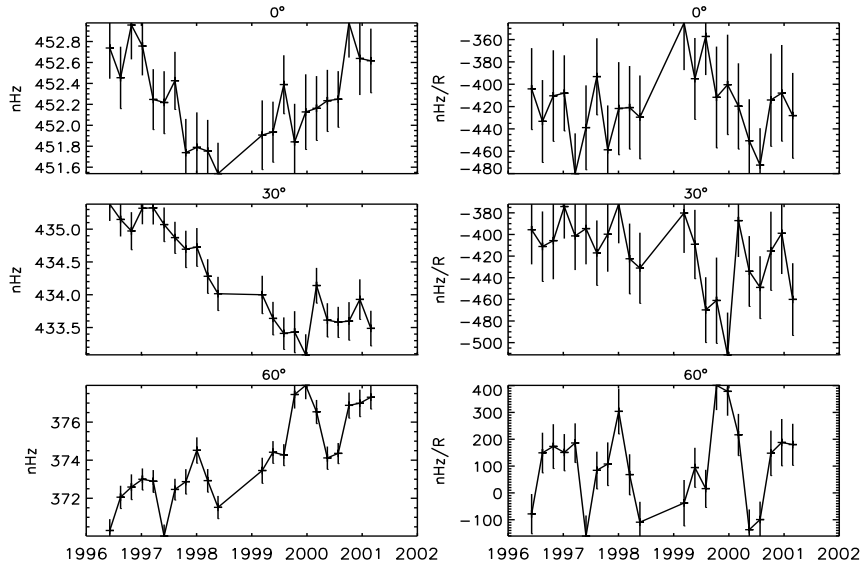


Figure 8. Intercept (left column) and slope (right column) of the linear fit Equation (7) at the equator, 30° and 60° of latitude (from top to bottom).

however. There is no noticeable annual variation in our inferred values of the surface rotation rate.

## 5. Discussion

We have used the depth and latitude variation in the sensitivities of the solar f modes to deduce the rotation profile in the subsurface shear layer of the Sun in the outer 15 Mm of the solar interior. Our work differs from earlier seismic investigations. These were either based on the f modes but implicitly assumed a depth-independent model of the rotation (e.g. Schou, 1999), or used global inversions of p- and f-mode splittings and consequently may suffer from any systematic difference between the p- and f-mode data (e.g. Schou et al., 1998), or used local helioseismic ring analysis (e.g. Basu et al., 1999; Haber et al., 2000), which promises to be a powerful diagnostic of near-surface flows and stratification but the sensitivity and systematics of which are still under investigation (Hindman et al. 2001, in preparation). By using just the splittings of the f modes, which are arguably the most straightforward helioseismic modes to interpret, we believe we are able to obtain not only a simple but also a clean measure of the near-surface shear. As with all inferences about rotation from global splittings, we note that

only that component of rotation which is symmetric about the equator is recovered.

The most robust results concern the low-latitude shear. The average gradient  $\partial \ln \Omega / \partial \ln r$  (at constant latitude) in the outer 15 Mm is close to  $-1$  and remarkably constant from the equator to  $30^\circ$  latitude. Between  $30^\circ$  and  $55^\circ$  latitude, the gradient is still negative but makes a steady transition to a small (absolute) value. All our analyses show this. The variation of rotation at these latitudes appears to be well described by a linear function of depth, within the outer 15 Mm.

As discussed in the Introduction, if moving parcels of fluid were to conserve their specific angular momentum as they moved towards or away from the rotation axis, one would find that the rotation rate varied as the inverse square of the distance from the axis of rotation, so at low latitudes one would have that  $\partial \ln \Omega / \partial \ln r \simeq -2$ . In reality other effects such as diffusion will cause exchange of angular momentum between parcels, so we may expect a logarithmic gradient somewhat smaller in magnitude than  $-2$ . A precise measurement of this value in the Sun provides information about the relative effectiveness of competing mechanisms transporting angular momentum. Our finding is that at latitudes below  $30^\circ$  the value of the logarithmic gradient is much closer to  $-1$  than to  $-2$ . In fact, this seems in reasonable agreement with the equatorial value found by DeRosa in numerical simulations of rotating compressible convective fluid in a thin shell representing the Sun between about  $0.94R$  and  $0.98R$  (DeRosa, 2001; DeRosa et al., 2001). Also these simulations show a tendency for the gradient to decrease in magnitude as one moves from equator to mid-latitudes, albeit at lower latitudes than we find for the Sun. Although these simulations exclude for numerical reasons the near-surface layers that we are probing, the qualitative agreement is nonetheless encouraging.

At latitudes above  $\sim 55^\circ$ , the depth-averaged gradient over the layer appears to change sign with respect to the low-latitude shear, though this is largely a consequence of the behaviour in the very near-surface layers (outer 5 Mm) which in turn is deduced from the splittings of the highest-degree  $f$  modes. The gradient in the range of depths 5 – 15 Mm is small at these high latitudes; and such significant gradient  $\partial \Omega / \partial r$  as does exist at high latitude (if any) is in the outer 5 Mm and predominantly positive. We note that, using a ring-analysis technique, Basu et al. (1999) deduced a similar behaviour at high latitudes, finding a reversal of gradient in a zone above  $0.994R_\odot$ .

Concerning the surface rotation rate itself, below  $55^\circ$  our extrapolation of the rotation rate to the surface is in satisfactory agreement with the directly measured spectroscopic surface rotation rate (cf. Table I). Our inferred surface rate should be more accurate than one simply

inferred from the averaged f-mode splittings, because we take out the linear gradient with depth which undoubtedly exists at these latitudes: this can make a difference of  $\sim 5$  nHz, even over the fairly small range of depths sampled by the observed f modes.

The seismically inferred surface rate at high latitudes is considerably less secure. It has previously been reported from helioseismic investigations that the high-latitude surface rate is lower what one would expect from a simple three-term extrapolation from lower latitudes (Schou et al., 1998; Schou, 1999). Indeed it can be seen from panel f of Figure 3 that many of the points fall below the extrapolated spectroscopic rate for that latitude, implying that the rotation rate at *some* depth is lower than the spectroscopic surface rate one would infer from the values in Table I. The rather flat plateau of values in those panels strongly suggests that the rotation rate at about 10-15 Mm depth is slower than the extrapolated spectroscopic rate, which is confirmed by our OLA inversion result at those depths. However, the combined splittings at high degree are *increasing* with  $l$  and if taken at face value, as is done in our OLA inversion result for  $r = 0.997R$ , this behaviour implies that the very near-surface rotation rate is actually higher than the spectroscopic rate. Thus the matter is still open. Since the quoted spectroscopic rate is principally an extrapolation of surface observations at low- and mid-latitudes, the true rotation rate that would be determined by spectroscopy at high latitudes is uncertain. Direct spectroscopic determinations at high latitude would resolve the question. The very high-degree splittings could contain some systematic errors, and if these affect the low- $m$  data the most (some evidence for such an effect for p modes at lower degrees is offered by the comparison of GONG and MDI splittings by Schou et al. (2001)), then the near-surface, high-latitude rotation rates inferred here could be erroneously high. We hope that this possibility will shortly be addressed by independent determinations of these splittings by the GONG experiment using the new higher-resolution GONG+ observations.

## 6. Conclusion

Finally, to return again to our principal focus which is the shear gradient of the near-surface rotation, we find that at low and mid-latitudes the gradient  $\partial\Omega/\partial r$  in the outer 15 Mm or so is close to  $-1$  and is quite independent of latitude below  $30^\circ$ ; between  $30^\circ$  and  $\sim 50^\circ$  latitude, it is still negative but makes a transition to small absolute value. At higher latitudes, the gradient in the bulk of the outer 15 Mm is probably small, but if the highest-degree ( $l > 250$ ) data are to be believed there



is a region of positive gradient in the outer 5 Mm at high latitudes, similar to what Basu et al. (1999) found from ring analysis. We find no evidence for the gradient to vary with time: the torsional oscillation seems to pass through without changing the shear gradient in the outer 15 Mm.

Interestingly, the most recent circulation-dominated dynamo models (Dikpati and Charbonneau, 1999; Küker et al., 2001) are able to reproduce to some extent the equatorward migration patterns without invoking any radial gradient of angular velocity at the surface. Such negative gradient at low latitude should however probably be taken into account because if it is associated with a positive surface  $\alpha$ -effect, it will compete against the surface poleward circulation and contribute to producing the equatorward migration of magnetic patterns observed at the surface of the Sun.

### Acknowledgements

We thank Marc DeRosa, Maussumi Dikpati, François Lignières and Peter Gilman for useful discussions. Prof. Juri Toomre and Dr. Steve Tomczyk are thanked for hospitality at JILA and HAO respectively where part of this work was carried out. The work was supported by the UK Particle Physics & Astronomy Research Council through the award of grant PPA/A/S/2000/00171.

### Appendix

#### Derivation of f-mode 1.5D kernels

The polynomial  $\mathcal{P}$  used to describe the frequency splittings can be expressed in terms of the Clebsh-Gordan coefficients  $C_{j_1 m_1 j_2 m_2}^{jm}$  (e.g. Edmonds, 1960) by:

$$\mathcal{P}_j^{(l)}(m) = \beta_j^l C_{lmj0}^{lm}; \quad \beta_j^l \equiv \frac{l\sqrt{(2l-j)!(2l+j+1)!}}{(2l)!\sqrt{2l+1}}. \quad (10)$$

The Gegenbauer polynomials used in Equation (2) are defined by (e.g. Morse and Feshbach, 1953):

$$T_{2j}^1(\mu) = \sqrt{\frac{4\pi}{4j+3}} \frac{\partial Y_{2j+1}^0(\theta, \phi)}{\partial \mu}. \quad (11)$$

From Ritzwoller and Lively (1991) we can deduce that

$$2\pi a_{2j+1}^l = \frac{v_{2j+1}^l}{T_{2j}^1(0)} \int_0^1 K_j^l(r) \Omega_{2j+1}(r) dr, \quad (12)$$

where  $v_{2j+1}^l \equiv L^2 C_{l1(2j+1)0}^{l1} / \beta_{2j+1}^l$ ,  $L^2 \equiv l(l+1)$  and

$$K_j^l(r) = \frac{(\xi_l^2 + (L^2 - 1 - j(2j+3))\eta_l^2 - 2\xi_l\eta_l) \rho r^2}{\int_0^1 (\xi_l^2 + L^2\eta_l^2) \rho r^2 dr}, \quad (13)$$

$\xi_l$  and  $\eta_l$  being respectively the radial and horizontal displacement eigenfunctions which are determined by solving the differential equations describing the motion of a self-gravitating fluid body in a standard solar model (e.g. Unno et al., 1989) and  $\rho$  is the density profile given by the model, all these being functions of the fractional solar radius  $r$ .

Other expressions of practical interest can be found for  $v_{2j+1}^l$  that are recalled here for completeness. Pijpers (1997) established the recurrence relation

$$v_{2j+1}^l = \frac{(j-l)(2j+1)}{j(2l+2j+1)} v_{2j-1}^l; \quad (14)$$

and Schou (1999) noticed that to a very good approximation

$$v_{2j+1}^l / T_{2j}^1(0) \approx e^{-j(j+3/2)/l}. \quad (15)$$

The f modes are horizontally propagating surface gravity waves for which the displacement eigenfunctions satisfy the following surface boundary condition under the Cowling approximation (e.g. Berthomieu and Christensen-Dalsgaard, 1991):

$$\eta_l(r) \approx \frac{g_s}{R_\odot w_l^2} \xi_l(r), \quad (16)$$

where  $g_s = GM_\odot/R_\odot^2$  is the surface gravitational acceleration. Moreover, the angular frequencies  $w_l = 2\pi\nu_{l0}$  of the f modes follow asymptotically (for  $l \rightarrow \infty$ ) the dispersion relation  $w_l^2 \approx g_s L/R_\odot$ . Therefore we have  $\xi_l \approx L\eta_l$  and, from Equation (13), the rotational kernels associated with the f modes can be written as a function of the horizontal displacement only:

$$K_j^l(r) \approx k_j^l K_h^l(r) \begin{cases} K_h^l(r) \equiv \frac{\eta_l(r)^2 \rho(r) r^2}{\int_0^1 \eta_l(r)^2 \rho(r) r^2 dr} \\ k_j^l \equiv 1 - \frac{1}{L} - \frac{1}{2L^2} (1 + j(2j+3)) \end{cases}. \quad (17)$$

Finally, Equation (3) is obtained by taking:

$$u_{2j+1}^l \approx k_j^l e^{-j(j+3/2)/l}. \quad (18)$$

We note that Equation (5) is obtained by using the fact that, in the approximation Equation (17) valid for f modes, the rotational kernels depend on  $j$  only by a multiplicative factor. Taking instead  $K_j^l \approx K_0^l$  for all  $j$  as usually done for high degree modes would also allow us to write Equation (5) but the integrated difference  $\int (K_j^l - K_0^l) dr$  would reach 2.2% for  $l = 117$ ,  $j = 17$  whereas it remains negligible for all  $l$  and  $j$  in the case of the approximation used here.

## References

- Antia, H. M., Basu, S., Pintar, J. and Schou, J.: 2001, in: A. Wilson (ed), *Helio- and Asteroseismology at the Dawn of the Millennium*, ESA Publications Division, Noordwijk, The Netherlands, SP-464, p. 27.
- Backus, G. E. and Gilbert, J. F.: 1968, *Geophys. J. Roy. Astron. Soc.* **16**, 169.
- Basu, S., Antia, H. M. and Tripathy, S. C.: 1999, *Astrophys. J.* **512**, 458.
- Beck, J. G.: 2000, *Solar Phys.* **191**, 47.
- Beck, J. G. and Schou, J.: 2000, *Solar Phys.* **193**, 333.
- Berthomieu, G. and Christensen-Dalsgaard, J.: 1991, in: A. N. Cox, W. C. Livingston and M. Matthews (eds.): *Solar Interior and Atmosphere*, The University of Arizona Press, Tucson, USA, p. 412.
- Birch, A. C. and Kosovichev, A. G.: 1998, *Astrophys. J.* **503**, L187.
- Brown, T. M., Christensen-Dalsgaard, J., Dziembowski, W. A., Goode, P., Gough, D. O. and Morrow, C. A.: 1989, *Astrophys. J.* **343**, 526.
- Christensen-Dalsgaard, J., Schou, J. and Thompson, M. J.: 1990, *MNRAS* **242**, 353.
- Collin, B., Nesme-Ribes, E., Leroy, B., Meunier, N. and Sokoloff, D.: 1995, *C.R. Acad. Sci. Paris* **321**, 111.
- Corbard, T., Berthomieu, G., Morel, P., Provost, J., Schou, J. and Tomczyk, S.: 1997, *Astron. Astrophys.* **324**, 298.
- Corbard, T., Jiménez-Reyes, S. J., Tomczyk, S., Dikpati, M. and Gilman P.: 2001, in: A. Wilson (ed), *Helio- and Asteroseismology at the Dawn of the Millennium*, ESA Publications Division, Noordwijk, The Netherlands, SP-464, p. 265.
- DeRosa, M. L.: 2001, Ph.D. thesis, University of Colorado, Boulder, USA.
- DeRosa, M. L., Gilman, P. and Toomre, J.: 2001, *Astrophys. J.* submitted.
- Deubner, F.-L., Ulrich, R. K. and Rhodes, E. J.: 1979, *Astron. Astrophys.* **72**, 177.
- Dikpati, M. and Charbonneau, P.: 1999, *Astrophys. J.* **518**, 508.
- Duvall, T. L.: 1980, *Solar Phys.* **66**, 213.
- Edmonds: 1960, *Angular Momentum in Quantum Mechanics*. Princeton University Press, Princeton, New Jersey, USA.
- Foukal, P.: 1972, *Astrophys. J.* **173**, 439.
- Foukal, P.: 1977, *Astrophys. J.* **218**, 539.
- Foukal, P. and Jokiipii, J. R.: 1975, *Astrophys. J.* **199**, L71.
- Gilman, P. A. and Foukal, P. V.: 1979, *Astrophys. J.* **229**, 1179.
- Gilman, P. A., Morrow, C. A. and Deluca, E. E.: 1989, *Astrophys. J.* **338**, 528.
- Haber, D. A., Hindman, B. W., Toomre, J., Bogart, R. S., Thompson, M. J. and Hill, F.: 2000, *Solar Phys.* **192**, 335.
- Hansen, C. J., Cox, J.P. and Van-Horn, H. M.: 1977, *Astrophys. J.* **217**, 151.
- Hathaway, D. H., et al.: 1996, *Science* **272**, 1306.
- Howard, R.: 1984, *ARA&A* **22**, 131.

- Howard, R. and Labonte, B. J.: 1980, *Astrophys. J.* **239**, L33.
- Howe, R., Christensen-Dalsgaard, J., et al.: 2000, *Astrophys. J.* **533**, L163.
- Küker, M., Rüdiger, G. and Schultz, M.: 2001, *Astron. Astrophys.* **374**, 301.
- Kosovichev, A. G. and Schou, J.: 1997, *Astrophys. J.* **482**, L207.
- Leighton, R. B.: 1969, *Astrophys. J.* **156**, 1.
- Morse, P. and Feshbach, H.: 1953, *Methods of Theoretical Physics, Vol. 1*, McGraw-Hill, New York, USA.
- Parker, E. N.: 1993, *Astrophys. J.* **408**, 707.
- Pijpers, F. P.: 1997, *Astron. Astrophys.* **326**, 1235.
- Ritzwoller, M. H. and Lavelly, E. M.: 1991, *Astrophys. J.* **369**, 557.
- Roberts, P. H. and Stix, M.: 1972, *Astron. Astrophys.* **18**, 453.
- Schou, J.: 1992, Ph.D. thesis, Aarhus University, Aarhus, Denmark.
- Schou, J.: 1999, *Astrophys. J.* **523**, L181.
- Schou, J., Christensen-Dalsgaard, J. and Thompson, M. J.: 1994, *Astrophys. J.* **433**, 389.
- Schou, J. et al.: 1998, *Astrophys. J.* **505**.
- Schou, J., Howe, R., et al.: 2001, *Astrophys. J.* submitted.
- Schroeter, E. H.: 1985, *Solar Phys.* **100**, 141.
- Snodgrass, H. B.: 1992, in: K. L. Harvey (ed.), *ASP Conf. Ser. 27: The Solar Cycle*, ASP, San Francisco, USA, p. 205.
- Snodgrass, H. B., Howard, R. and Webster, L.: 1984, *Solar Phys.* **90**, 199.
- Snodgrass, H. B. and Ulrich, R. K.: 1990, *Astrophys. J.* **351**, 309.
- Thompson, M. J., Toomre, J., et al.: 1996, *Science* **272**, 1300.
- Unno, W., Osaki, Y., Ando, H., Saio, H. and Shibahashi, H.: 1989, *Nonradial oscillations of stars, 2nd ed.*, University of Tokyo Press, Tokyo, Japan.